

Supplementary informations

Thermal variation of the lattice parameter from neutron diffraction and XRD

In Figure S1, is shown typical Rietveld refinement of powder neutron pattern using Fullprof software. We show the neutron and X-ray patterns obtained in the different temperature ranges respectively in Fig. S2 and S3. The lattice parameters and fitting quality factors are reported in Table S1. For comparison, we also show the lattice parameters obtained by DFT calculations from structural relaxation. These calculated lattice parameters are in close agreement with our previous calculations [S1].

In Table S3, we report the thermal variation of the different interatomic distances obtained from the Rietveld refinement of the neutron data. The results from DFT calculations are shown for comparison. The largest interatomic distances found in DFT calculations are consistent with the largest lattice parameters.

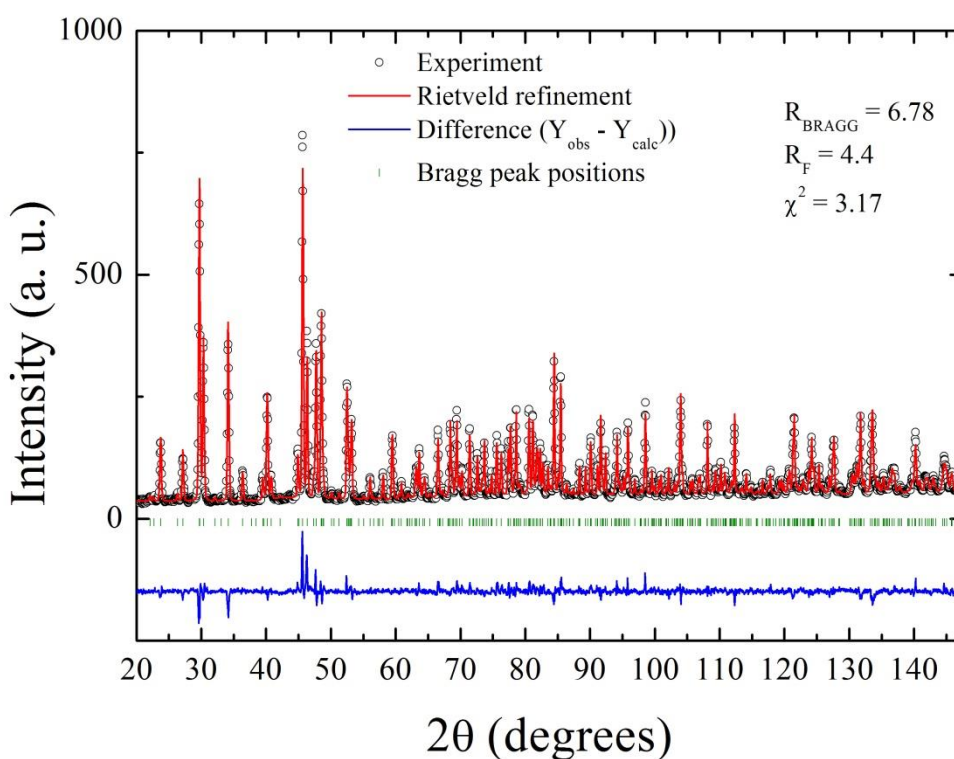


Fig. S1: Neutron diffraction pattern of ZnSb at 300 K (circles) with results of Rietveld refinement (red solid line), difference between calculated and observed curves (blue line) and Bragg peak positions (blue vertical bars)

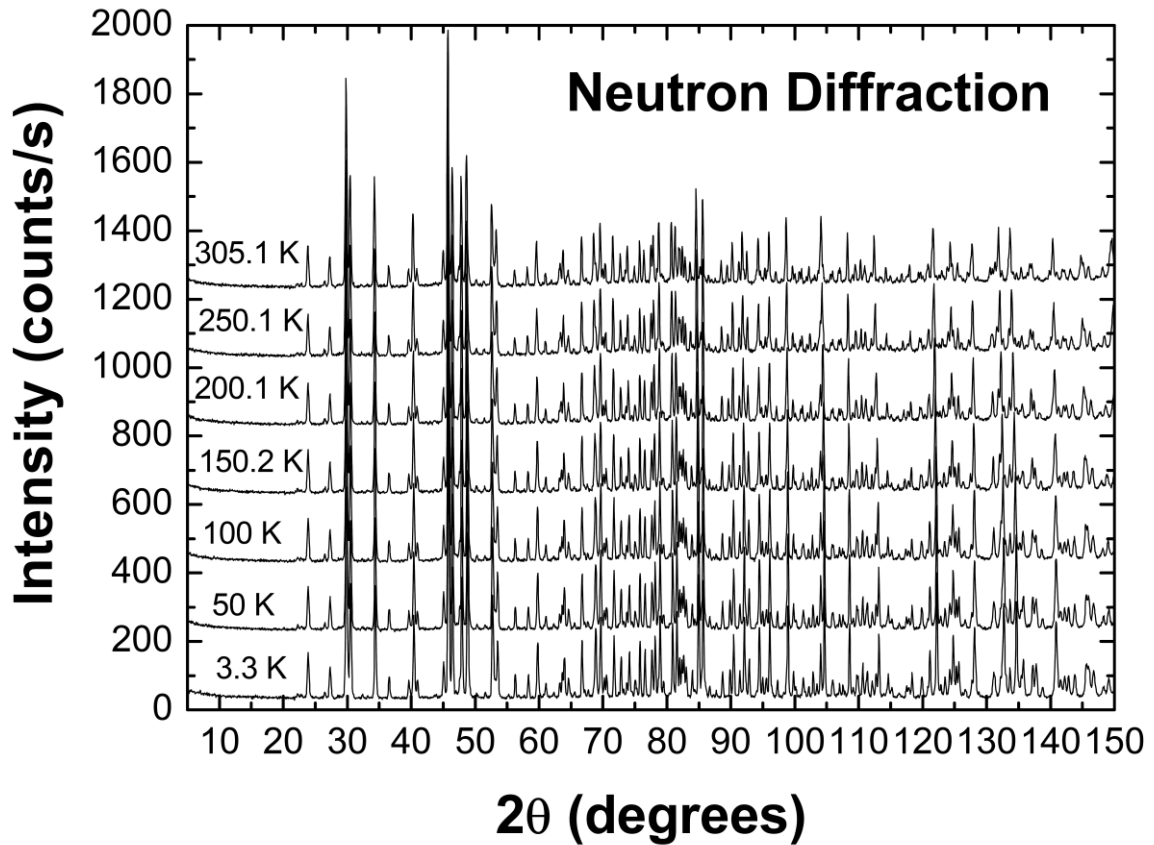


Fig. S2: Neutron diffraction pattern of ZnSb at different temperatures

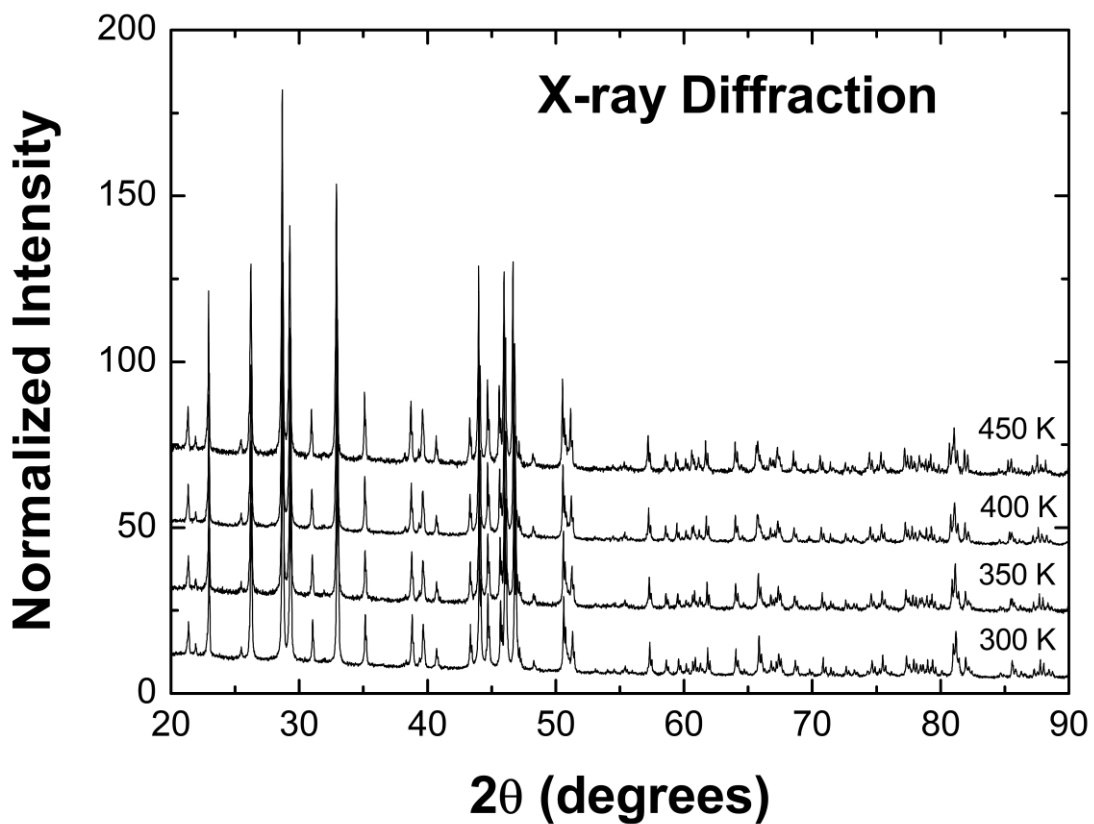


Fig. S3: X-ray diffraction pattern of ZnSb at different temperatures

T (K)	a (Å)	b (Å)	c (Å)	V (Å ³)	χ^2	R _{Bragg}	R _F
0 (DFPT)	6.289911	7.830829	8.237307				
3.3	6.17364(3)	7.72654(4)	8.09414(4)	386.098(3)	3.96	5.58	3.21
50	6.17486(3)	7.72664(4)	8.09389(4)	386.167(3)	3.98	5.69	3.18
100	6.17906(3)	7.72829(4)	8.09422(4)	386.526(3)	3.74	5.83	3.29
150.2	6.18430(3)	7.73114(4)	8.09535(4)	387.052(4)	3.7	6.38	3.69
200.1	6.19006(3)	7.73477(4)	8.09682(5)	387.665(4)	3.47	6.49	3.93
250.1	6.19604(3)	7.73859(5)	8.09844(5)	388.309(4)	3.43	6.77	4.08
305.1	6.20301(4)	7.74304(5)	8.10041(5)	389.064(4)	3.17	6.78	4.4

Table S1: Lattice parameters and refinement quality parameters from Rietveld refinement of neutron diffraction experiments.

T (K)	x _{Zn}	y _{Zn}	z _{Zn}	x _{Sb}	y _{Sb}	z _{Sb}
0 (DFPT)	0.041927	0.107525	0.12776	0.358357	0.417554	0.390885
3.3	0.04079(17)	0.10947(13)	0.12917(14)	0.35660(16)	0.41764(15)	0.39147(13)
50	0.04095(17)	0.10941(13)	0.12925(15)	0.35643(16)	0.41764(15)	0.39149(13)
100	0.04112(17)	0.10967(13)	0.12913(15)	0.35628(16)	0.41756(16)	0.39142(14)
150.2	0.04188(18)	0.10989(14)	0.12920(17)	0.35653(17)	0.41778(16)	0.39140(14)
200.1	0.04213(19)	0.11023(14)	0.12923(17)	0.35636(17)	0.41764(17)	0.39157(15)
250.1	0.04250(20)	0.11019(15)	0.12944(19)	0.35655(19)	0.41792(17)	0.39168(15)
305.1	0.04287(20)	0.11049(16)	0.12956(20)	0.35640(18)	0.41798(17)	0.39159(16)

Table S2: Atom positions determined from Rietveld refinement of neutron diffraction experiments.

T (K)	d _{S1-S2} (Å)	d _{Z3-S1} (Å)	d _{Z1-S1} (Å)	d _{Z4-S1} (Å)	d _{Z2-S1} (Å)	d _{Z2-Z4} (Å)
0 (DFPT)	2.8415	2.6928	2.7026	2.7942	2.9285	2.7466
3.3	2.8003(16)	2.6440(15)	2.6656(16)	2.7472(16)	2.8712(15)	2.7364(16)
50	2.8016(16)	2.6454(16)	2.6650(16)	2.7462(16)	2.8714(15)	2.7371(16)
100	2.8050(16)	2.6446(16)	2.6671(17)	2.7457(16)	2.8743(16)	2.7389(17)
150.2	2.8030(17)	2.6472(17)	2.6657(18)	2.7456(17)	2.8817(16)	2.7443(20)
200.1	2.8051(18)	2.6466(17)	2.6694(18)	2.7446(18)	2.8865(17)	2.7493(19)
250.1	2.8021(18)	2.6510(18)	2.6675(19)	2.7461(18)	2.8908(17)	2.753(2)
305.1	2.8057(18)	2.6526(19)	2.668(2)	2.7472(19)	2.8959(18)	2.760(2)

Table S3: Thermal variation of the nearest-neighbor interatomic distances in ZnSb determined from Rietveld refinement of neutron diffraction experiments.

There are 20 different types of angles in ZnSb. Below one shows only the angles varying significantly with the temperature.

Case of Zn-Sb-Zn angles

There are 6 different types of Zn-Sb-Zn angles. The two (Z1-S1-Z3) and (Z1-S1-Z4) angles do not show significant variation with increasing temperature. The (Z3-S1-Z4) angle of about 106.4° very slightly increases with increasing temperature but within the error. As can be seen in Figure S4, only the Zn-Sb-Zn angles implying the longest intra-ring Z2-S1 interatomic distances show significant thermal variation. Note that the intra-ring (Z2-S1-Z4) angle increases from 58.25° to 58.5° with increasing temperature.

Case of Sb-Zn-Sb angles

There are 6 different types of Sb-Zn-Sb angles. The two (S4-Z4-S5) and (S1-Z4-S5) angles slightly increase and the (S3-Z4-S5) angle slightly decreases with increasing temperature, but within the error. The remaining Sb-Zn-Sb angles vary significantly with increasing temperature as shown in Figure S4. Note that the wide intra-ring (S3-Z4-S1) angle decreases from 121.75° to 121.5° with increasing temperature.

Case of Zn-Zn-Sb angles and Zn-Sb-Sb

There are 4 different types of Zn-Zn-Sb angles and also 4 different types of Sb-Sb-Zn angles. Among these last ones, the inter-ring (Z1-S1-S2) angle does not show significant variation with temperature. The temperature variation of the other angles is reported in Figure S5. It is significant that the two narrow intra-ring (Z2-Z4-S1) and (Z2-Z4-S3) Zn-Zn-Sb angles have very strong temperature dependence with opposite behavior and all the Zn-Zn-Sb angles have strong temperature dependence.

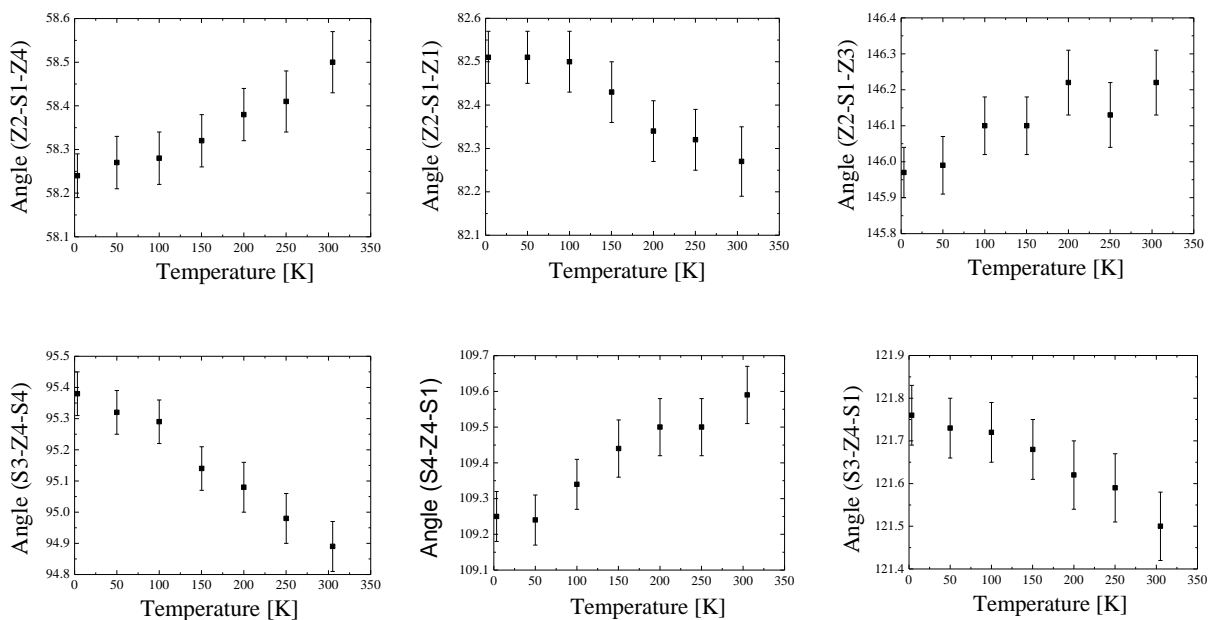


Fig. S4: Thermal variation of several Zn-Sb-Zn and Sb-Zn-Sb angles in ZnSb.

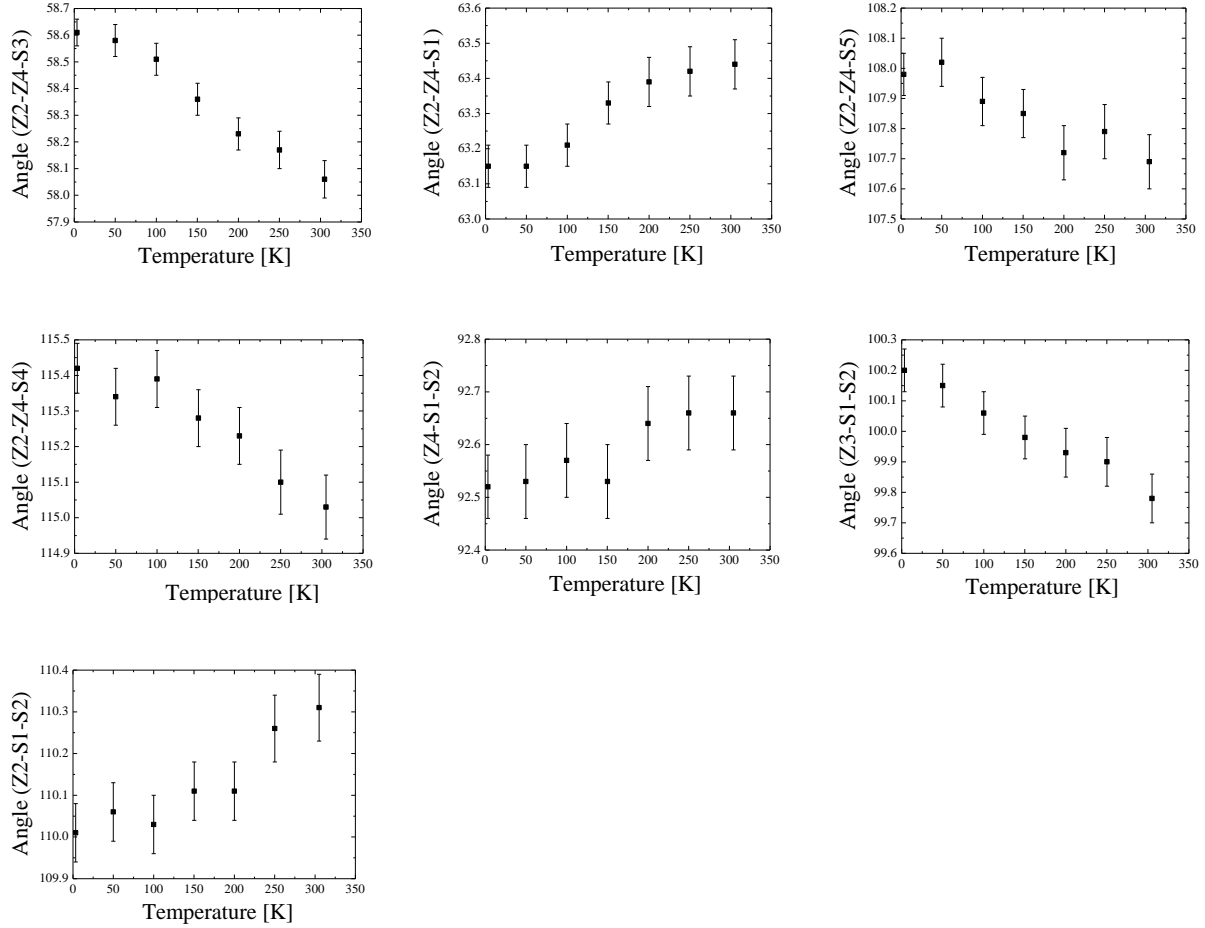


Fig. S5: Thermal variation of several Zn-Zn-Sb and Sb-Sb-Zn angles in ZnSb.

Elastic constants from DFPT calculations

c_{11}	c_{22}	c_{33}	c_{12}	c_{13}	c_{23}	c_{44}	c_{55}	c_{66}
81.37	92.77	80.94	30.09	29.07	26.26	18.45	36.69	28.99

Table S4: Elastic constants of ZnSb from DFPT calculations (in GPa)

One can see the very good agreement of the elastic constants calculated by DFPT with prior finite difference calculations [S1,S3]. The reader can use the formula in ref. S1 to obtain the related elastic constants.

Sound velocity and Debye temperature from DFPT calculations and Balazyuk's data [S4]

In an orthorhombic system, one can relate the velocities of the acoustical waves as following [S5]:

$$c_{11} = (\rho v_{la})^{1/2}; c_{22} = (\rho v_{lb})^{1/2}; c_{33} = (\rho v_{lc})^{1/2}; \\ c_{44} = (\rho v_{tbc})^{1/2} = (\rho v_{tcb})^{1/2}; c_{55} = (\rho v_{tac})^{1/2} = (\rho v_{ta})^{1/2}; c_{66} = (\rho v_{tab})^{1/2} = (\rho v_{tba})^{1/2} \quad (S-1)$$

In the anisotropic case, one can determine the sound velocity, v_{si} , and Debye temperature, θ_{Di} , for each i direction as done usually for the isotropic case (see e. g. ref. [S1] or [S5]).

	v_{la}	v_{tab}	v_{tac}	v_{lb}	v_{tbc}	v_{lc}	v_{sa}	v_{sb}	v_{sc}
DFPT	3571.3	2131.5	2398	3813.1	1700.7	3561.9	2475.6	2098.6	2159.4
Exp.	3805.6	2376.4	2693.9	4021.9	1839.1	3830.9	2752.8	2287.5	2355

Table S5: Sound velocities of ZnSb for different crystallographic directions from DFPT calculations and experiment [S4] (in m/s)

One can remark that v_{tbc} corresponding to transverse velocity is by far the lowest sound velocity and this explains why the sound velocity is lower following b and c directions.

	θ_{Da}	θ_{Db}	θ_{Dc}
DFPT	251	212.8	218.9
Exp.	282.9	235.1	242

Table S6: Debye temperatures of ZnSb for different crystallographic directions from DFPT calculations and experiment [S4] (in K)

One must note that we find different θ_{Di} Debye temperatures for ZnSb than in Anatychuk's work [S6]. These last authors have determined the θ_{Di} Debye temperatures from thermal variation of X-ray diffraction experiments. It is more reliable to determine them from the elastic constants.

Grüneisen parameter

The experimental thermodynamic Grüneisen parameters, Γ_i , for each i direction, have been determined from equ. (4) of the main paper.

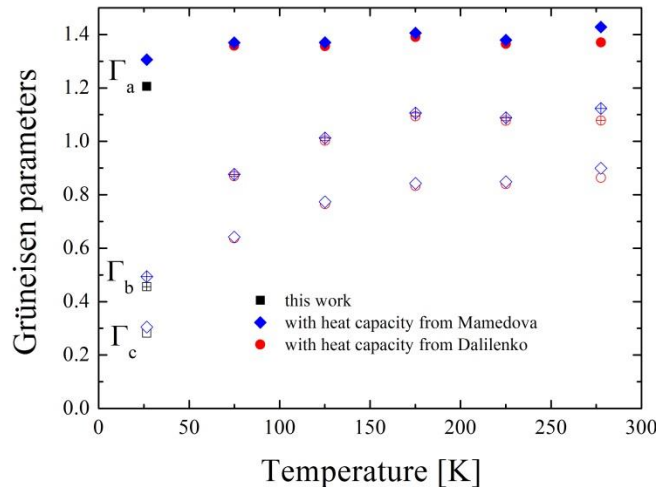


Fig. S6: Thermal variation of the thermodynamic Grüneisen parameters Γ_i from our thermal expansion and heat capacity, the heat capacity experiments [S8,S9] and elastic constant experiments [S4] in the literature.

The volume thermodynamic Grüneisen parameter, Γ , has been determined from [S7]:

$$\Gamma(T) = \sum_i \chi_i \Gamma_i / \chi \quad (\text{S-3})$$

where Γ_i and χ_i are respectively the Grüneisen parameters and compressibilities for each i direction and χ is the volume compressibility.

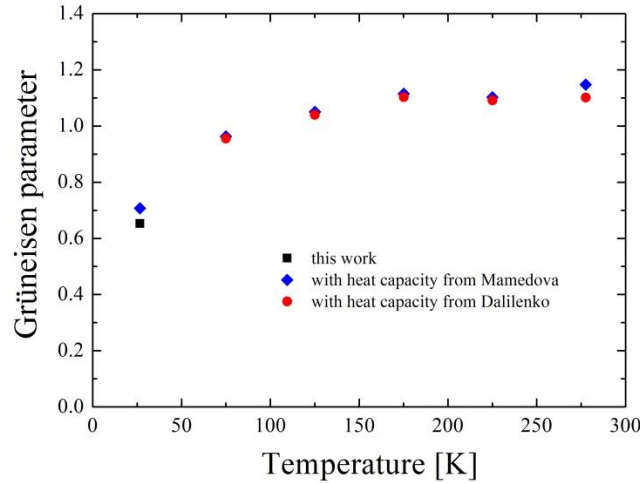


Fig. S7: Thermal variation of the volume thermodynamic Grüneisen parameters Γ from our thermal expansion and heat capacity, the heat capacity experiments [S8,S9] and elastic constant experiments [S4] in the literature.

References

- [S1] P. Jund, R. Viennois, X. Tao, K. Niedziolka, J. C. Tedenac, Phys. Rev. B **85**, 224105 (2012)
- [S2] B. C. Sales, D. G. Mandrus, B. C. Chakoumakos, Semicond. Semimetals **70**, 1 (2001)
- [S3] Note that, in ref. [S1], the two lines of table IV concerning the Cauchy pressures P_x^{Cauchy} and P_z^{Cauchy} have been reversed. One must read: $P_x^{\text{Cauchy}} = 7.44 \text{ GPa}$ and 9.5 GPa ; $P_z^{\text{Cauchy}} = -0.66 \text{ GPa}$ and 3.11 GPa .
- [S4] V. N. Balazyuk, A. I. Eremenko, N. D. Raransky, Funct. Mater. **15**, 343 (2008)
- [S5] J. Feng, B. Xiao, J. Chen, Y. Du, J. Yu, R. Zhou, Mater. Des. **32**, 3231 (2011)
- [S6] L. I. Anatychuk, V. P. Mikhachenko, J. of Thermoelectricity **13**, 21 (2002)
- [S7] T. H. K. Barron, J. G. Collins, G. K. White, Adv. Phys. **29**, 609-730 (1980)
- [S8] G. N. Danilenko, V. Ya. Shevchenko, S. F. Marenkin, M. Kh. Karapetyants, Inorg. Mat. **14**, 486 (1975)
- [S9] K. M. Mamedova, A. Yu. Dzhangirov, O. I. Dzhafarov, V. N. Kostryukov, Russ. J. Phys. Chem. **49**, 1635 (1975)